

Research Article

Relative Humidity Dependent Resistance Switching of Bi_2S_3 Nanowires

Raimonds Meija,¹ Gunta Kunakova,¹ Juris Prikulis,¹ Justin M. Varghese,²
Justin D. Holmes,² and Donats Erts^{1,3}

¹*Institute of Chemical Physics, University of Latvia, Raina Blvd. 19, Riga LV-1586, Latvia*

²*Centre for Research on Adaptive Nanostructures and Nanodevices, Trinity College, Dublin, Ireland*

³*Department of Chemistry, University of Latvia, Raina Blvd. 19, Riga LV-1586, Latvia*

Correspondence should be addressed to Raimonds Meija; raimonds.meija@lu.lv

Received 10 August 2017; Revised 4 November 2017; Accepted 29 November 2017; Published 25 December 2017

Academic Editor: Ilaria Armentano

Copyright © 2017 Raimonds Meija et al. This is an open access article distributed under the Creative Commons Attribution License, which permits unrestricted use, distribution, and reproduction in any medium, provided the original work is properly cited.

Electrical properties of Bi_2S_3 nanowires grown using a single source precursor in anodic aluminum oxide templates are sensitive to the relative humidity in an inert gas environment. Dynamic sensing dependency is obtained and shows presence of spontaneous resistance switching effect between low and high relative humidity states. Employing the thermionic field emission theory, heights of Schottky barriers are estimated from the current-voltage characteristics and in relation to the humidity response. The change of Schottky barrier height is explained by local changes in physically adsorbed water molecules on the surface of the nanowire.

1. Introduction

During the last decade, remarkable attention has been devoted to the applications of semiconductor nanowires in chemical sensor, resistive memory, and other electrical devices [1, 2]. Increased surface to volume ratio of nanowires improves their sensitivity to changes in the surrounding medium, which is useful for chemical sensor applications [3]. For example, Cui et al. demonstrated highly sensitive real-time biological sensors [4]. Peng et al. investigated NO sensing properties of porous silicon nanowires in dry air at room temperature [5]. In addition, resistive switching events have been observed and explained by different mechanisms including space charge limited current [6] and oxygen vacancy model [2, 7]. However, more detailed studies are needed to establish well controlled working principles of these devices and properties, especially of narrow band gap nanostructures, such as Bi_2S_3 nanowires.

The superior sensing behavior at nanoscale can also affect nonsensing devices, where nanostructures serve as building elements with certain well defined electrical properties.

Extreme oxygen sensitivity effect on carbon nanotube resistance was reported [8]. Jie et al. observed considerable impact of the air and humidity on the n-type silicon nanowires and even change in the p-type characteristics [9]. Therefore, sensing properties must be considered to advance the performance for most of the nanowire based applications. For example, exposure of metal oxide nanowire sensors to gaseous molecules can modify the density of oxygen vacancies [10]. On the other hand, drift of these vacancies has been found as one of the basic mechanisms for the memristive devices [2]. Consequently, studies of resistive switching may lead to improvements of established sensing effects.

Previous works on nanowire memory devices cover a wide range of oxide materials. Other solids including sulfur based nanowires are also considered to possess the resistive switching. For example, Ag_2S nanowires were found to show such effect at temperature of 10 K by formation of rupture of the connection with silver electrodes [11]. Similarly, random access memory devices have been presented by modulation of the Schottky barrier depletion region in Bi_2S_3 nanoplates [12]. Bi_2S_3 is an n-type semiconductor with a 1.3 eV direct band

gap. Conductivity of individual nanowires and nanowire arrays is well characterized [13–17]. Its characteristic doping with sulfur vacancies could be altered by the surface adsorbents governing remarkable change of resistance. This approach has a potential for applications in memory devices [14, 18]. It has also been shown that if the temperature is above 160 K, Bi_2S_3 nanowires exhibit either Schottky or Ohmic conductance mechanisms. However, below 160 K the space charge limited current is the dominant conduction mechanism for Bi_2S_3 nanowires [14].

In this work, we report on properties of Bi_2S_3 nanowires for possible applications as resistive memory and sensing devices. We focus on the working environment of the nanowire resistors at room temperature, which is the most common operating environment, with main emphasis on the relative humidity impact on the nanowire electrical properties. Unusual response to the relative humidity was found for individual Bi_2S_3 nanowire resistors, where reversible switching of the resistance is modulated by different RH levels.

2. Materials and Methods

Thermolysis of single source precursor bismuth bis(diethylthiocarbamate) [$\text{Bi}(\text{S}_2\text{CNET}_2)_3$] was used to deposit Bi_2S_3 in a porous anodic aluminum oxide (AAO) template forming single crystal nanowires with the mean diameters from 20 to 200 nm and length up to several tenths of micrometers. Detailed growth of the Bi_2S_3 nanowire arrays and compositional characterization is described elsewhere [19]. Mechanical polishing of both sides of AAO membrane was done to remove bulk crystallites formed during the synthesis. Polished nanowire-filled membranes were dissolved in a 9% H_3PO_4 solution in water. Obtained nanowire suspension was centrifuged to separate nanowires from the alumina dissolution products. Separated nanowires were washed in deionized water three times and then transferred to the isopropanol [14, 16].

In order to localize the nanowires on the surface, freshly prepared suspension was drop-casted on a silicon substrate coated with a 380 nm thick layer of SiO_2 (boron doped, SiMat) with prefabricated Au macroelectrodes. Electron beam lithography (Raith, Elphy Quantum, coupled with a scanning electron microscope (SEM) Hitachi S4800) was used for nanowire electrode deposition. For metallization, Ti/Au layers were evaporated in the precision etching and coating system (Gatan 682 PECS). Prior to measurements the fabricated devices were cleaned in oxygen plasma for 1 min, 30 W (Harrick plasma).

Electrical measurements were performed with a current-voltage source meter system, Keithley 6430 and 6487. Relative humidity sensitivity was measured in a custom made system with a controllable humidity level in argon (99.99%). Constant humidity level during experiments was provided using water-glycerol solutions [20]. All humidity sensing experiments were realized in the humid/dry argon with a flow of $2 \text{ cm}^3/\text{min}$. Level of the relative humidity and temperature inside the measurement chamber was monitored using a humidity sensor (Honeywell HIH-4010).

MATLAB based software PKUMSM.m [21] was used to determine the change of Schottky barrier heights from IVCs (applied parameters: $E_0 = 25 \text{ meV}$, $E_{00} = 1 \text{ meV}$, $R_{\text{sh}1} = R_{\text{sh}2} = 10^{15} \Omega$).

3. Results and Discussion

A typical Bi_2S_3 nanowire extracted from AAO and lithographically connected to metal electrodes is shown in Figure 1(a). Measured current-voltage characteristics (IVC) have nonlinear symmetric, asymmetric, or rectifying dependence and in Figure 1(b) we show example of nonlinear and symmetric IVC. The thermionic field emission theory based model for metal (M)–semiconductor (S)–metal (M) system with two corresponding Schottky barriers at M/S interface was used to approximate the obtained nonlinear IVCs for Bi_2S_3 nanowires (detailed process in [21, 22]). As one can see the simulated IVC (example in Figure 1(b), solid line) fits well the experimental data. Therefore, formation of the nonlinear IVCs can be explained by presence of Schottky barriers at Bi_2S_3 -Ti/Au contacts [22]. Determined values of extracted Schottky barriers are in order of 0.3–0.6 eV. These values correspond well with the previously reported data for Bi_2S_3 nanowire devices with Pd contacts [13].

Assuming ideal M/S contact, the height of Schottky barrier $\phi_{\text{Bi}_2\text{S}_3}$ can be roughly estimated as $\phi_{\text{Bi}_2\text{S}_3} = \phi_{\text{M}} - \chi$, where ϕ_{M} is the work function of the metal and χ is the electron affinity of the semiconductor [23]. Previously determined χ for Bi_2S_3 thin films is 4.5 eV [24]. Using the value of work function of Ti, which interface the Bi_2S_3 nanowires ($\phi_{\text{M}} = 4.6 \text{ eV}$ [25]) expected height of the Schottky barrier is in order of 0.1 eV. However, experimentally determined values of $\phi_{\text{Bi}_2\text{S}_3}$ are higher and this difference may be attributed to the presence of thin layer of native bismuth oxide on the nanowire surface.

Referring to our previous research on reproducible contact engineering for Bi_2S_3 nanowires, ohmic or Schottky barrier contacts can be produced using contact area etching before metal evaporation [15]. Thus, by removing or preserving the native oxide layer, one can select the type of the nanowire contact. In this work, we selected the ones with oxide layer enabled Schottky contacts, because, for the ohmic contacts, no resistive switching was observed.

To characterize the Bi_2S_3 nanowire relative humidity dependent electrical properties, IVCs were measured under RH-argon environment. Figures 2(a) and 2(b) demonstrate IVCs for two individual nanowires after exposure to different relative humidity levels. It was found that IVC has a hysteretic behavior with spontaneous resistance switching (RS) effect after exposure to low and high RH levels. The nanowire first was conditioned at 5% RH level for ~5 min (Figure 2(a) (curve-1)); then it was kept at 65% RH level (Figure 2(a) (curve-2)) for the same amount of time and IVC was obtained. 65% RH level was chosen, because, at $\text{RH} < 60\%$, no resistive switching events could be observed. The duration of one IVC measurement was 2 minutes. At a low initial conditioning RH level, the measured IVCs did not exhibit any hysteresis and forward-reverse biased voltage sweeps resulted in similar current values. However, after RH level was

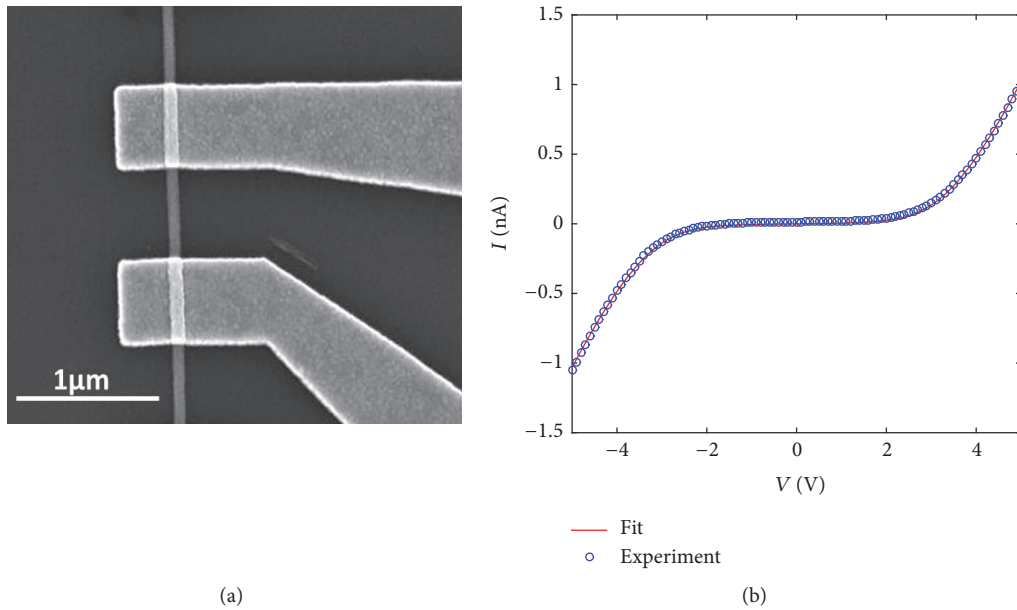


FIGURE 1: Electrical characterization of individual Bi_2S_3 nanowires: (a) SEM image of connected Bi_2S_3 nanowire ($d_{\text{NW}} \approx 80$ nm); (b) IVC of Bi_2S_3 nanowire with nonlinear dependence; solid fit corresponds to simulated IVC with two reverse Schottky barriers; extracted Schottky barrier height $\phi_1 \approx \phi_2 = 0.6$ eV; relative humidity level = 5%.

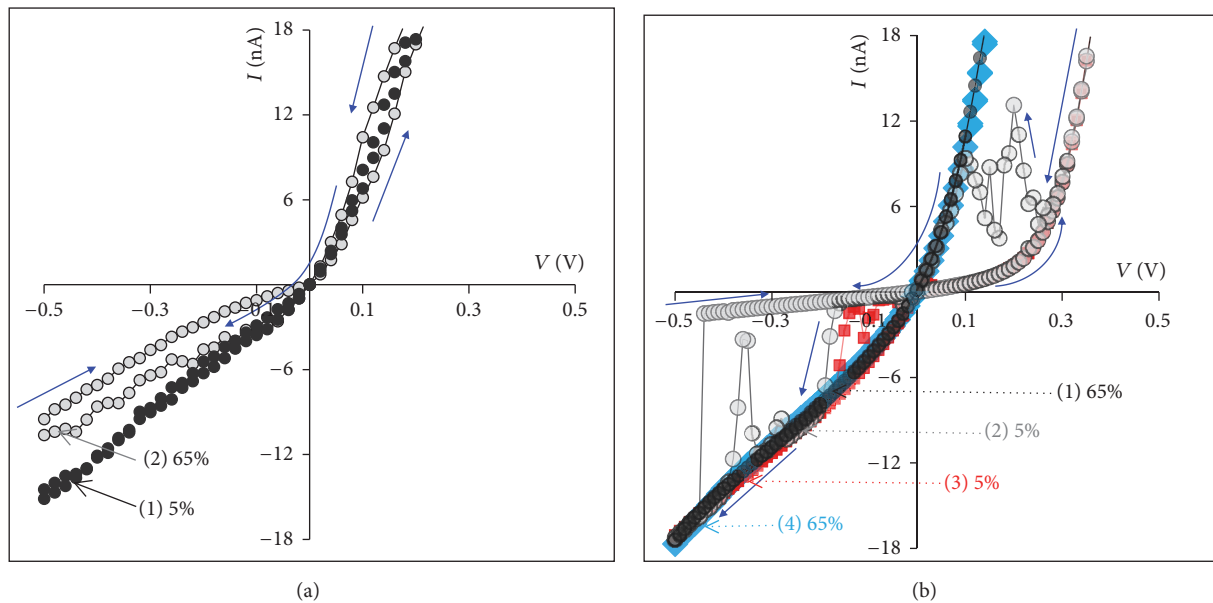


FIGURE 2: (a), (b) IVCs of the Bi_2S_3 nanowires measured at argon atmosphere with low (5%) and increased (65%) relative humidity level; notations (1) to (4) indicate the sequence of IVC capturing.

increased, the repeated IVC (Figure 2(a), (curve-2)) exhibited hysteresis with occasional jumps back to the same path as for nonhysteretic curves measured at low RH. The sequence was repeated in a reversed order for another nanowire (initial high RH followed by low RH) and even stronger effect of

resistive switching was observed (Figure 2(b)). It can be seen that the IV curves in Figures 1(b) and 2 are different. It can be attributed to different Schottky barrier heights for different nanowires, as described in [22]. The magnitude of the RS can vary from nanowire to nanowire, as one can see

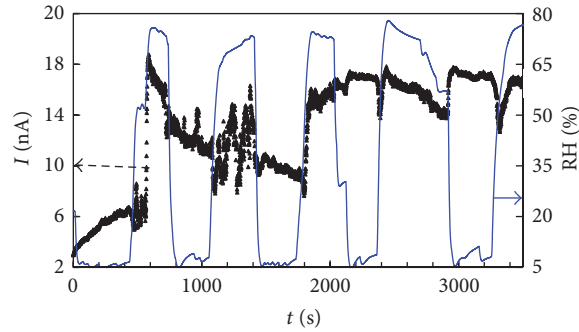


FIGURE 3: Dynamic response of the current of individual Bi_2S_3 nanowire modulated by ~ 5 and 75% RH levels under constant applied voltage (300 mV).

by comparing these two devices in Figures 2(a) and 2(b). We believe that this is due to nonhomogeneity of the oxide layer on top of the nanowire forming the Schottky barrier once interfacing the metal contact. To obtain nanowire devices with reproducible RS events, more effort needs to be done by engineering reproducible Schottky barrier contacts. It is also worth pointing out that, in terms of individual nanowire, the IVCs after the RH exposure are consistent and the random resistive switching events can be repeated. In Figure 2(b), curve-3 is measured under the same conditions as curve-2 (right after capturing curve-2), also showing RS. To confirm that the RH exposure cycles did not damage the nanowire, curve-4 was measured after ~ 1 h reconditioning in room conditions (with a RH $\sim 65\%$). As one can see, the IVC follows the same path as the first captured curve-1. In addition to IVCs, for selected experiments, nanowires were controlled visually using SEM technique.

Different IVC capturing sequences, that is, 5 to 65% and 65 to 5%, correspond to conditions with water molecule adsorption and desorption processes. Poorly visible RS events for 5–65% process and very well pronounced ones for the reversed 65–5% IVC capturing sequence (Figures 2(a) and 2(b)) indicate that the RS events could be most likely induced by an incomplete water molecule desorption process. To better understand this effect, we measured the dynamic current response.

The dynamic time dependent current response was measured under constant bias voltage after exposure to fast changes of RH, 5% \rightarrow 75% \rightarrow 5% (Figure 3). After exposure to the 75% RH, the current of the nanowire cannot be recovered to the initial RH values of 5%. When the RH is changed from 5% to 75% for the second time, chaotic jumps of the current were observed (Figure 3).

The water molecule adsorption-desorption process on the nanowire surface can be assumed as a relatively slow process and one could expect that incomplete water molecule adsorption (desorption) initiated the observed RS.

The presence of the Schottky barrier is a key ingredient to induce/observe the RS for Bi_2S_3 nanowires. Captured nonlinear IVCs (Figure 4(b)) were used to determine the

height of the Schottky barriers at different RH levels. We have plotted extracted $\phi_{\text{Bi}_2\text{S}_3}$ versus relative humidity level as shown in Figure 4(a). The Schottky barrier does not change significantly at RH levels below 60%, but at higher RH levels the value of $\phi_{\text{Bi}_2\text{S}_3}$ starts to increase. This corresponds to the RH diapason, where the $\phi_{\text{Bi}_2\text{S}_3}$ remains constant. Therefore, observed increase in barrier height at RH $> 60\%$ can explain the change in IVCs, as can be seen in Figure 2(a).

When the RH levels are relatively small ($\ll 60\%$), only a chemisorbed layer is formed on the surface of the nanowire (Figure 4(c)). When the RH levels increase above 60%, then also on top of chemisorbed layers water is sorbed physically and both the Schottky barrier and the depletion region width increase (Figure 4(d)). This means that the nanowire is less conductive. As the physisorbed layer is not very stable, physically adsorbed water molecules can locally regroup and change the width of the depletion layer and height of Schottky barrier, which may explain the resistive switching at RHs above 60% (Figures 3 and 4).

4. Conclusions

We have demonstrated relative humidity dependent resistance switching effect for Bi_2S_3 nanowires in inert gas atmosphere. Dependence of the Schottky barrier height versus RH indicates significant increase in the Schottky barrier at RH values above 60%.

The current-voltage characteristics of the Bi_2S_3 nanowires at constant relative humidity levels in argon show resistive switching events. They can be attributed to the immobile (chemisorbed) and mobile (physisorbed) water molecules layer formation on the nanowire surface, which locally change the height of the Schottky barrier and depletion layer width. Consequently, at high RH level uncontrolled desorption and local regrouping of the physisorbed water molecules can occur and resist drop to the value corresponding to low RH level. Further investigation of the water molecule adsorption effects on the Bi_2S_3 nanowire surface is needed to fully utilize the switching effect in functional devices.

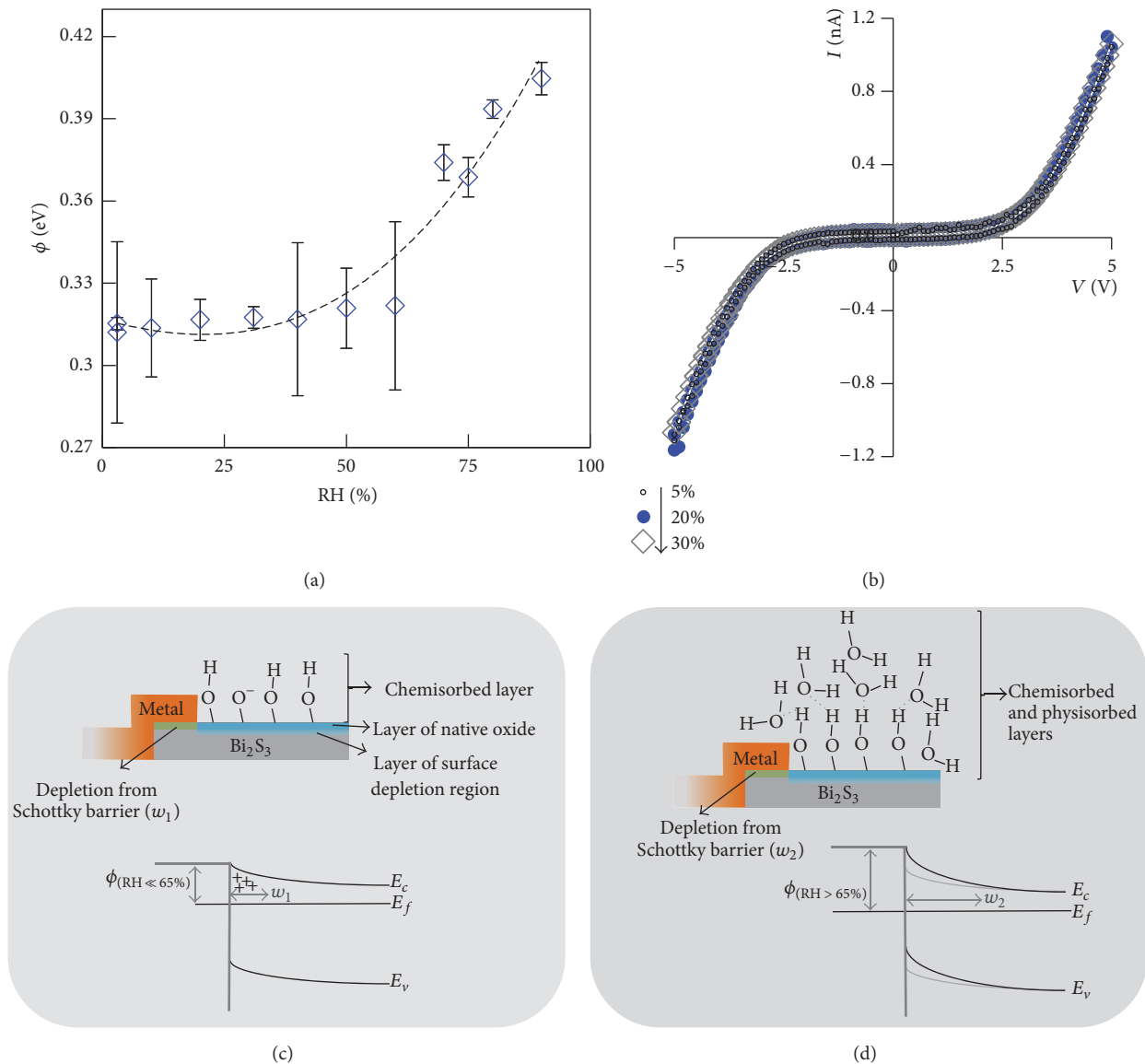


FIGURE 4: (a) Determined values of $\phi_{\text{Bi}_2\text{S}_3}$ versus relative humidity; (b) IVCs at RH levels 5, 20, and 30%; arrow indicates IVC capturing sequence; (c), (d) schematic representation for the modulation of $\phi_{\text{Bi}_2\text{S}_3}$ under low ($\text{RH} \ll 60\%$) and high ($\text{RH} > 60\%$) relative humidity levels.

Conflicts of Interest

The authors declare that there are no conflicts of interest regarding the publication of this paper.

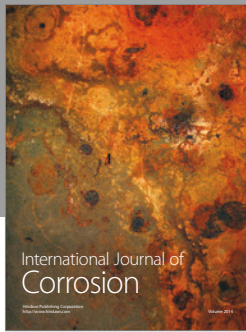
Acknowledgments

This work was done within Latvian National Research Program IMIS 2 and University of Latvia Base/Performance Funding Projects nos. AAP2016/B043 and ZD2010/AZ19.

References

- [1] S.-H. Bae, S. Lee, H. Koo et al., "The memristive properties of a single VO_2 nanowire with switching controlled by self-heating," *Advanced Materials*, vol. 25, no. 36, pp. 5098–5103, 2013.
- [2] J. J. Yang, M. D. Pickett, X. Li, D. A. A. Ohlberg, D. R. Stewart, and R. S. Williams, "Memristive switching mechanism for metal/oxide/metal nanodevices," *Nature Nanotechnology*, vol. 3, no. 11, pp. 429–433, 2008.
- [3] J. Du, D. Liang, H. Tang, and X. P. A. Gao, "InAs nanowire transistors as gas sensor and the response mechanism," *Nano Letters*, vol. 9, no. 12, pp. 4348–4351, 2009.
- [4] Y. Cui, Q. Wei, H. Park, and C. M. Lieber, "Nanowire nanosensors for highly sensitive and selective detection of biological and chemical species," *Science*, vol. 293, no. 80, pp. 1289–1292, 2001.
- [5] K.-Q. Peng, X. Wang, and S.-T. Lee, "Gas sensing properties of single crystalline porous silicon nanowires," *Applied Physics Letters*, vol. 95, Article ID 243112, 2010.
- [6] Y. Xia, W. He, L. Chen, X. Meng, and Z. Liu, "Field-induced resistive switching based on space-charge-limited current," *Applied Physics Letters*, vol. 90, p. 022907, 2007.

- [7] D. B. Strukov, J. L. Borghetti, and R. Stanley Williams, "Coupled ionic and electronic transport model of thin-film semiconductor memristive behavior," *Small*, vol. 5, no. 9, pp. 1058–1063, 2009.
- [8] G. C. Philip, B. Keith, I. Masa, and A. Zettl, "Extreme oxygen sensitivity of electronic properties of carbon nanotubes," *Science*, vol. 287, no. 5459, pp. 1801–1804, 2000.
- [9] J. Jie, W. Zhang, K. Peng, G. Yuan, C. S. Lee, and S.-T. Lee, "Surface-dominated transport properties of silicon nanowires," *Advanced Functional Materials*, vol. 18, no. 20, pp. 3251–3257, 2008.
- [10] P.-C. Chen, F. N. Ishikawa, H.-K. Chang, K. Ryu, and C. Zhou, "A nanoelectronic nose: a hybrid nanowire/carbon nanotube sensor array with integrated micromachined hotplates for sensitive gas discrimination," *Nanotechnology*, vol. 20, no. 12, Article ID 125503, 2009.
- [11] Z. Liao, C. Hou, H. Zhang, D. Wang, and D. Yu, "Evolution of resistive switching over bias duration of single Ag₂S nanowires," *Applied Physics Letters*, Article ID 203109, pp. 2–5, 2010.
- [12] G.-Y. Liu, L.-Y. Xu, F. Zhou et al., "Dynamic random access memory devices based on bismuth sulfide nanoplates prepared from a single source precursor," *Physical Chemistry Chemical Physics*, vol. 15, no. 27, pp. 11554–11558, 2013.
- [13] K. Yao, Z. Y. Zhang, X. L. Liang, Q. Chen, L.-M. Peng, and Y. Yu, "Effect of H₂ on the electrical transport properties of single Bi₂S₃ nanowires," *The Journal of Physical Chemistry B*, vol. 110, no. 43, pp. 21408–21411, 2006.
- [14] G. Kunakova, R. Viter, S. Abay et al., "Space charge limited current mechanism in Bi₂S₃ nanowires," *Journal of Applied Physics*, vol. 119, no. 11, Article ID 114308, 2016.
- [15] G. Kunakova, J. Katkevics, A. Viksna et al., "Electrical characterisation of Bi₂S₃ nanowire arrays by electrochemical impedance spectroscopy," *Electrochimica Acta*, vol. 170, pp. 33–38, 2015.
- [16] G. Kunakova, R. Meija, I. Bite et al., "Sensing properties of assembled Bi₂S₃ nanowire arrays," *Physica Scripta*, vol. 90, no. 9, Article ID 094017, 2015.
- [17] J. Katkevics, G. Kunakova, A. Viksna, J. D. Holmes, and D. Erts, "Impedance and admittance characteristics of Bi₂S₃ nanowire arrays," in *Proceedings of the International Conference on Functional Materials and Nanotechnologies 2013 (FM and NT '13)*, vol. 49, April 2013.
- [18] D. Guo, C. Hu, and C. Zhang, "First-principles study on doping and temperature dependence of thermoelectric property of Bi₂S₃ thermoelectric material," *Materials Research Bulletin*, vol. 48, no. 5, pp. 1984–1988, 2013.
- [19] J. Xu, N. Petkov, X. Wu et al., "Oriented growth of single-crystalline Bi₂S₃ nanowire arrays," *Physical Chemistry Chemical Physics*, vol. 8, no. 2, pp. 235–240, 2007.
- [20] C. F. Forney and D. G. Brandl, "Control of humidity in small controlled- environment chambers using glycerol-water solutions," *Horttechnology*, vol. 2, pp. 52–54, 1992.
- [21] Y. Liu, Z. Y. Zhang, Y. F. Hu, C. H. Jin, and L. Peng, "Quantitative fitting of nonlinear current-voltage curves and parameter retrieval of semiconducting nanowire, nanotube and nanoribbon devices," *Journal of Nanoscience and Nanotechnology*, vol. 8, no. 1, pp. 252–258, 2008.
- [22] Z. Zhang, K. Yao, Y. Liu et al., "Quantitative analysis of current-voltage characteristics of semiconducting nanowires: decoupling of contact effects," *Advanced Functional Materials*, vol. 17, no. 14, pp. 2478–2489, 2007.
- [23] R. F. Pierret, *Semiconductor Device Fundamentals*, Addison—Wesley Publishing Company, 2nd edition, 1996.
- [24] E. Pineda, M. E. Nicho, P. K. Nair, and H. Hu, "Optoelectronic properties of chemically deposited Bi₂S₃ thin films and the photovoltaic performance of Bi₂S₃/P3OT solar cells," *Solar Energy*, vol. 86, no. 4, pp. 1017–1022, 2012.
- [25] H. L. Skriver and N. M. Rosengaard, "Surface energy and work function of elemental metals," *Physical Review B: Condensed Matter and Materials Physics*, vol. 46, no. 11, pp. 7157–7168, 1992.



Hindawi

Submit your manuscripts at
<https://www.hindawi.com>

